J Mol Model (2017) 23: 222
DOI 10.1007/s00894-017-3391-z

ORIGINAL PAPER

The functionalization of carbon nanotubes to enhance the efficacy of the anticancer drug paclitaxel: a molecular dynamics simulation study

Hassan Hashemzadeh[1] · **Heidar Raissi**[1]

Received: 28 January 2017 / Accepted: 22 June 2017 / Published online: 12 July 2017

Abstract Carbon nanotubes (CNTs) are widely used in drug delivery systems (DDSs) due to their unique chemical and physical properties. Investigation of interactions between biomolecules and CNTs is an interesting and important subject in biological applications. In this study, we used molecular dynamics (MD) simulation to investigate the adsorption mechanism of the anticancer drug paclitaxel (PTX) on pristine and functionalized CNTs (*f*-CNT) in aqueous solutions. Our theoretical results show that PTX can be adsorbed on sidewalls of CNT in different methods. In the case of *f*-CNTs, PTX can be adsorbed on the functional groups due to the existence of polar interactions. These interactions in the CNT functionalized with polyethylene glycol (PEG), are more than the other investigated systems. Furthermore, it was found that the solubility of CNTs in aqueous solution is increased by functionalization. This is related to the intermolecular hydrogen bonds between functional groups and solvent molecules. The PEG group has the greatest effect on the solubility of the CNT in aqueous solution due to more polar interactions.

Keywords Paclitaxel anticancer drug · Molecular dynamics simulation · Functionalized carbon nanotube · Solubility carbon nanotube · Drug delivery system

Electronic supplementary material The online version of this article (doi:10.1007/s00894-017-3391-z) contains supplementary material, which is available to authorized users.

✉ Hassan Hashemzadeh
hashemzade_h@birjand.ac.ir

Heidar Raissi
hraeisi@birjand.ac.ir

[1] Department of Chemistry, University of Birjand, Birjand, Iran

Introduction

Today, cancer is one of the key causes of mortality in modern societies. A variety of anticancer drugs have been employed in cancer treatment, but most of these drugs have systemic toxicity and low therapeutic effectiveness with acute side effects [1–3]. PTX is a strong anticancer drug for the treatment of a wide range of cancers. However, the use of this drug is limited due to very low solubility in aqueous solutions and high severe side effects [4].

Today, many systems based on drug delivery have been developed to enhance bioavailability and reduce side effects of anticancer drugs. There are several types of nanoparticles, such as polymeric nanoparticles, CNTs, and nanocrystals that can be used as DDSs for the PTX drug molecule. The encapsulation of PTX in these biodegradable and non-toxic nano-DDSs can enhance the PTX solubility, improve PTX pharmacokinetic profiles in vivo, and decrease its side effects [5]. Generally, one of the best carriers for drug delivery are CNTs as they can bind to the drug molecules through covalent or noncovalent interactions [6]. This type of DDS can improve the therapeutic performance of the drug molecules. Since the pristine CNTs are chemically inert and do not dissolve in solvents, covalent or non-covalent functionalization is usually required to render them soluble, and also to attach other chemical moieties. These modifications can alter the CNT properties, such as the selectivity, biocompatibility, solubility, and decrease toxicity and retention in the tumor [7].

Lay et al. reported that modification of CNTs with PEG groups leads to improved cytotoxicity of PTX in cancer cells and enhances their solubility. They also found that modified CNTs can be used as DDSs to improve bioavailability and efficacy of insoluble drugs [8].

Arsawang et al. performed MD simulation to provide more insight into the structural properties of the encapsulation of gemcitabine in the single-walled carbon nanotubes (SWNT).

Their obtained results indicated that the drug molecule prefers to locate inside the SWNT, and the formation of π-π stacking interaction between the cytosine ring of drug and CNTs is the main interaction in the encapsulation of the drug [9]. Li et al. reported MD simulation results for the vinblastine (VLB)-CNT interactions in different conditions. Free energy results reveal that the drug molecule can take three stable orientations on the CNT sidewall under the attachment of loading mode. Furthermore, they found that functionalization of the CNT with ester groups enhanced the biocompatibility of drug with biological systems and reduced the toxicity of the CNT [10].

Mousavi et al. performed steered molecular dynamics (SMD) to investigate the penetration mechanisms of carbon nanotube (CNTs)-encapsulated PTX, through the phospholipid bilayer membrane. They found that the CNT facilitates targeted delivery of the polar PTX molecule through the lipid bilayer since it has the ability to penetrate into the cell membrane. Their results show that the van der Waals and hydrogen bond (HB) interactions are the main interactions in the delivery of PTX molecules [11].

Despite the existence of numerous experimental studies on the CNTs (the pristine and modified CNTs) based on PTX delivery [8, 12], there are few theoretical reports that investigate the interactions between this drug and CNT. Therefore, it's necessary to provide a thorough understanding of these systems and improve the performance of the DDSs. Such theoretical studies can provide fundamental knowledge for the design and optimization of the CNT-based carriers for the PTX delivery.

In the present work, we investigated and compared the adsorption mechanism of the PTX anticancer drug on the pristine and functionalized CNTs. Functionalization of the CNT was done using carboxylic (−COOH), CH_2NH_2 (−AMINE) and -PEG groups. PEG is a biocompatible polymer, which can be conjugated with CNTs and has attractive advantages such as extension blood circulation time of CNTs by reducing the amount of their uptake by the reticuloendothelial system (RES) [7]; it also enhances dispersion and biocompatibility of CNTs etc. Furthermore, we examined the adsorbed orientation of the PTX molecule on sidewalls of CNT. Finally, comprehensive investigations have been done on the role of functional groups on solubility of CNTs in aqueous solutions. The evaluation of the effect of several functional groups on the DDS performance and the PTX solubility distinguishes our study from the other investigations. The results of this work can give an insight into the effect of functional groups on CNT-based DDS, which could be helpful in future experimental studies by medical scientists.

Methods

Preparation of structures

An armchair (12, 12) SWNT with a diameter of 1.61 *nm* and the length of 4 *nm* was selected as the model carrier. The CNT was first generated from the Nanotube Modeler package [13] and then functionalized with -COOH, −PEG (contain 12 monomer [14]), and -AMINE groups in four sites at two entrances of CNT (Fig. 1 shows the structure of pristine CNT and *f*-CNTs from the front and side view).

The geometry of the PTX molecule has been optimized at the B3LYP/6-31G* level of theory as implemented in GAMESS package and partial charges on each atom have been obtained from these DFT calculations [15]. The chemical structure of the PTX molecule is shown in Fig. 2.

It should be noted that in all investigated systems (pristine CNT and *f*-CNTs) the PTX molecules were located around the outer surface of CNT and separated sufficiently far away (> 3 nm) to eliminate the effect of starting orientations [16].

Force fields

The force fields parameters for CNT, functional groups, and PTX, were taken from the Charmm27 force field [17]. The bond stretching is described by the following equation:

$$U(b) = K_b(b-b_0)^2 \quad (1)$$

Where K_b, and b, are the bond force-constant and the bond length, respectively. The subscript zero represents the equilibrium values for the individual terms.

While the angle bending is given by:

$$U(\theta) = K_\theta(\theta-\theta_0)^2 \quad (2)$$

Where K_θ and θ are the angle force constants and bond angle, respectively.

The torsional potential in the CNT is given by:

$$U(\varphi) = K_\varphi(1 + cos(n\varphi-\delta)) \quad (3)$$

Where K_φ and φ are dihedrals force constants and dihedral angles, respectively, n is the multiplicity and δ is the phase, which dictates the location of the minima and maxima.

Finally, nonbonded interactions are calculated based on the Lennard-Jones potential, according to the expression:

$$U(r_{ij}) = \varepsilon_{ij}\left[\left(\frac{\sigma_{ij}}{r_{ij}}\right)^{12} - 2\left(\frac{\sigma_{ij}}{r_{ij}}\right)^{6}\right] \quad (4)$$

In Eq. (4), $\varepsilon_{ij} = \sqrt{\epsilon_{ii}\epsilon_{jj}}$ is the well depth, where i and j are the indices of the interacting atoms, r_{ij} is the interatomic distance, and $\sigma_{ij} = \frac{1}{2}(\sigma_{ii}\sigma_{jj})$ is the distance at which the LJ term has its minimum. Table S1 shows the values for LJ parameters in the non-bond interaction for CNT and functional groups.

Based on previous works [18, 19], the CNT atoms were modeled as uncharged Lennard–Jones particles. The topology of PTX for application in MD simulations was taken from the SwissParam server [20]. It should be noted that, the input file

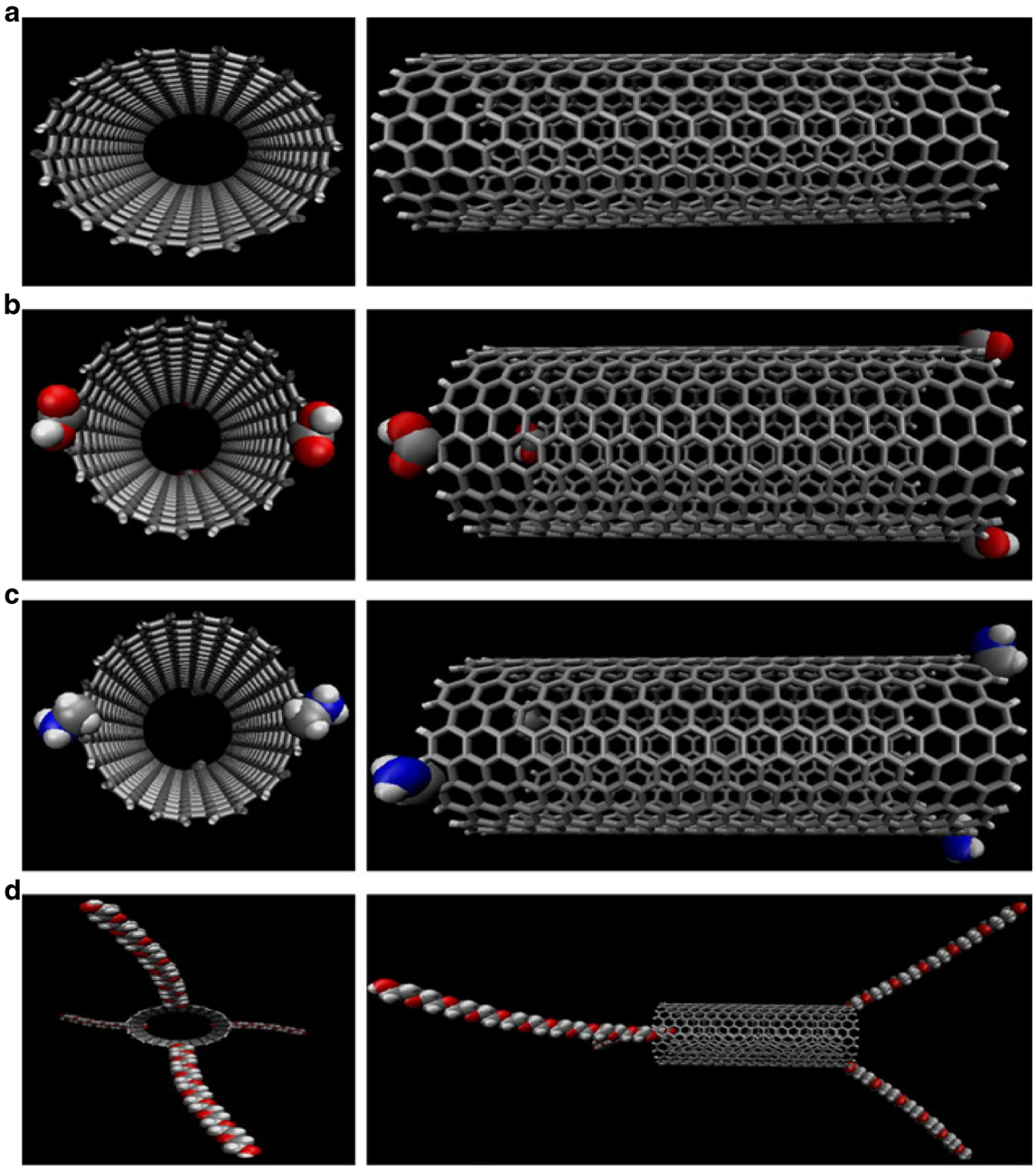

Fig. 1 Schematic structure of the pristine CNT and *f*-CNTs from the front and side view (a) pristine CNT (b) COOH-CNT (c) AMINE-CNT (d) PEG-CNT

for SwissParam in mol2 format was constructed from optimized PTX structure. The TIP3P model was used for simulating the water molecules in all systems [21].

Free energy

Solvation free energies were calculated by the thermodynamic integration method [22] based on a series of MD simulations carried out using the GROMACS software. In GROMACS, the Hamiltonian of the solution is decomposed into solute-solute, solute-solvent, and solvent-solvent contributions. A coupling parameter, λ, is applied to the solute-solvent part of the Hamiltonian, so that its contribution can be modulated between full interactions (corresponding to $\lambda = 0$) and no interactions ($\lambda = 1$). This particular implementation obviates the need for a separate calculation of a single solute in vacuum to account for the contribution of intramolecular solute-solute interactions, via a thermodynamic cycle.

In thermodynamic integration, independent simulations are carried out for different values of λ, between 0 and 1, and the gradient of the Hamiltonian with respect to λ is

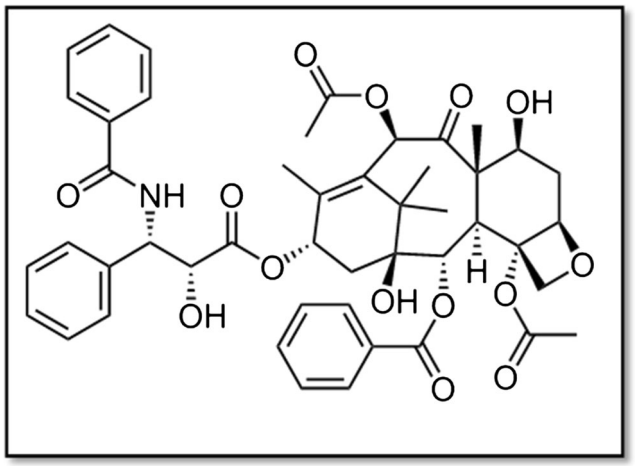

Fig. 2 Paclitaxel (PTX) structure

averaged over a large number of equilibrated configurations. The solvation free energy (ΔG_{sol}) is then calculated by numerically integrating the Hamiltonian gradient over l, following Eq. (5):

$$\Delta G_{sol} = \int_0^1 < \frac{\partial H(p,q,\lambda)}{\partial \lambda} > d\lambda \quad (5)$$

Where H is the Hamiltonian of the system, which depends on the particle positions (q) and momenta (p), as well as on the coupling parameter.

Simulation

In this work, molecular dynamics simulation was performed using the GROMACS 4.5.5 MD simulation package [23]. Body temperature is 310 K and for this reason the MD simulation was performed at this temperature. The temperature was maintained by applying the V-rescale thermostat and the pressure was kept constant at 1 *bar* using the Berendsen algorithm [24]. The equations of motion were solved using the leap-frog algorithm under periodic boundary conditions and the simulation was carried out for the total time of 150 *ns*.

For all systems, the dimensions of the simulation box were set as 7 *nm* × 7 *nm* × 13 *nm*. LINCS algorithm was used to constrain all bonds in all of the systems. The particle-mesh Ewald (PME) method was used to treat long-range electrostatic interactions while electrostatic interactions between charged groups Lenard-Jones (L-J) interactions were calculated with a 1.4 *nm* range cutoff. Grid algorithm was used to search neighbors. The visual molecular dynamics (VMD) program has been used for molecular visualization [25]. The initial and final structures of investigated systems with 5 PTX molecules have been shown in Fig. 3 from top and side view.

Results

Mechanism of adsorption

The equilibrium state and the stability of the structure during MD simulations can be evaluated by several quantities such as the potential and total energy, root mean-squared deviation (RMSD), the pressure of the systems, etc. [19, 26]. Figsures S1 and S2 (Supplementary material) show **RMSD** and **total energy** curves, respectively, for all of the investigated systems. The results indicated that all of the systems reached the equilibrium state after 1 *ns*.

Radial distribution function (RDF) for all systems in the first 10 ns of simulations was calculated to analyze the characteristics of interactions. The RDF represents the probability of finding atom *i* at a spherical shell of a certain distance (r) from the atom *j*. A sharp peak in the RDF plots is attributed to the interaction between two groups. The RDF for PTX molecules around the surface of CNTs was calculated and given in Fig. 4a. According to the obtained results, the main amounts of interactions between PTX molecules and CNTs exist at a distance of approximately 0.5–2.2 *nm* and the maximum interactions occur at 0.92 and 2.08 *nm*. Based on pervious works [9, 10], these peaks can be related to formation of the π–π stacking interactions between aromatic rings of PTX molecules and sidewalls of CNTs. Also, the polar interactions, such as partial π–π interactions and hydrogen bonds (HBs), which can be formed between the functional groups of CNTs and the heteroatoms of PTX, are other reasons for this observation.

It is noteworthy that the most intense peak is observed in the PEG-CNT system, which shows that this system has more interaction with PTX than the other systems. The RDF of water molecules around the surface of CNTs have been calculated and shown in Fig. 4b. It is obvious that the lowest intensity peak is related to the PEG-CNT system. This result confirms that increasing the interaction of CNT and drug leads to the repulsion of water molecules from the CNT.

To understand the molecular orientation of PTX adsorbed on CNTs, we calculated the atomic RDF of drug molecules. The calculated atomic RDF for the drug molecules are given in Fig. 5a. It is observed that the sharp peaks for the aromatic ring atoms (CA and HA atoms) and amine groups (N and HN atoms) are located at 0.50 and 0.70 *nm*, while the wide peaks for other atoms (CR, CO, OC, HO, and HC) are located between 0.80 and 1.10 *nm*. These results show that the PTX molecules with their aromatic rings are adsorbed on sidewalls of CNT, which emphasizes that the π-π stacking between the PTX and the CNT surface plays the major role in drug adsorption. Furthermore, it is interesting to note that the oxygen atoms of drug are oriented away from the CNTs

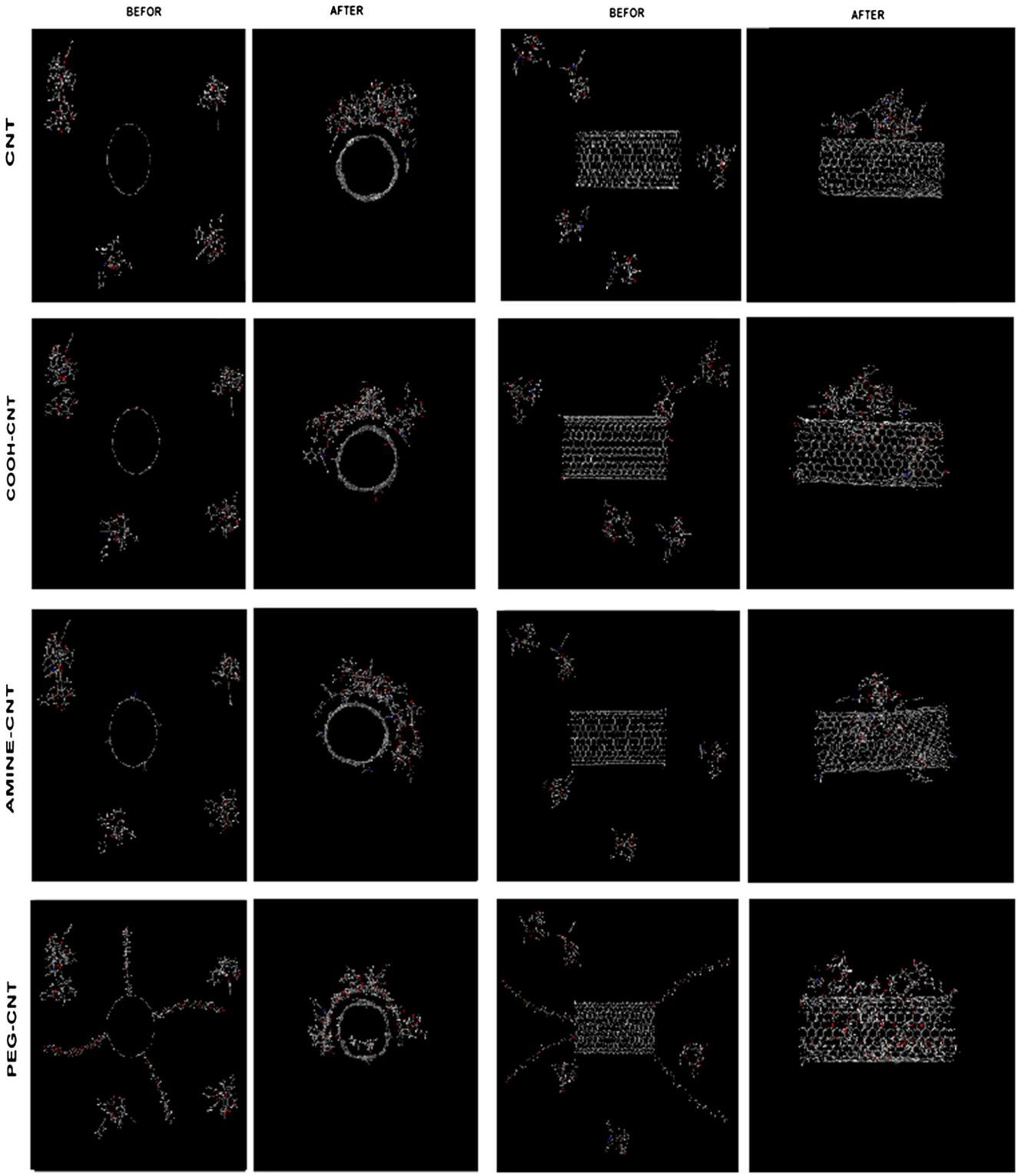

Fig. 3 Initial and final snapshots of different systems as obtained from the MD simulation. Water molecules are not shown for clarity

and toward the aqueous phase to enhance the solubility of DDS in water solution. According to these results, our suggested schematic model for the orientation of adsorption of PTX molecule on PEG-CNT is shown in Fig. 5b.

To study the geometry of π–π stacking interactions, we calculated the distance between the CNT surface and the aromatic rings of PTX. The schematic view of the distance between CNT and PTX is provided in Fig. S3.

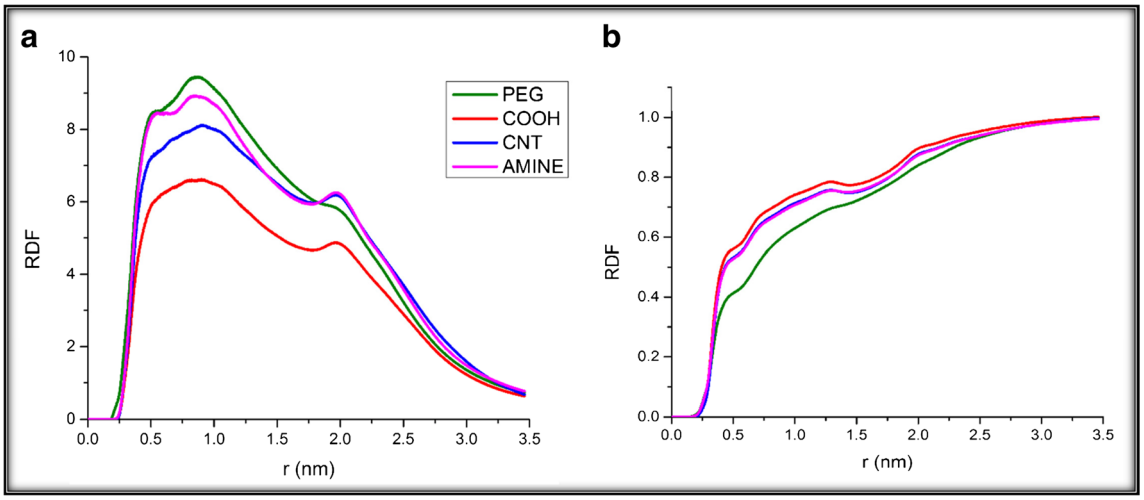

Fig. 4 (a) Radial distribution functions (RDF) between PTX and CNTs (b) RDF of water molecules around CNT(red), COOH-CNT(blue), AMINE-CNT(pink), and PEG-CNT(green)

Fig. 5 **a)** Atomic RDF between PTX atoms and PEG-CNT b) schematic model for the orientation of PTX on PEG-CNT

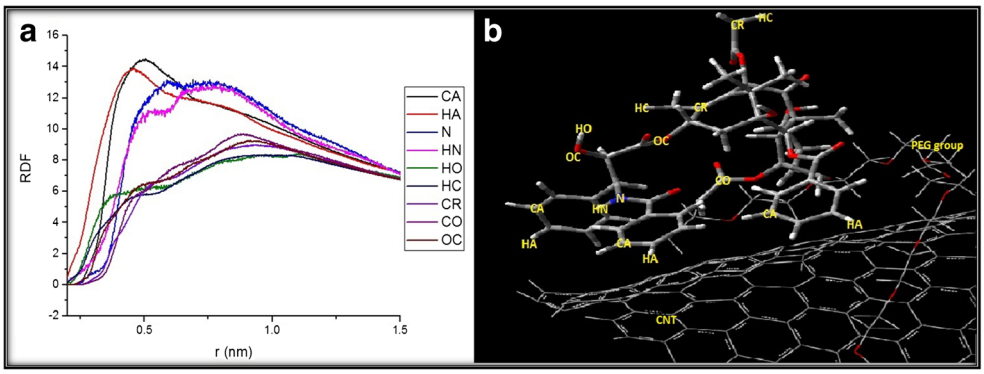

There are two types of π stacking interactions between aryl groups of PTX and CNT surface, T-shaped and parallel π-π stacking interactions with 2.87 A° and 3.57–3.93 A° from the CNT sidewall, respectively. In parallel orientation, the aromatic rings of PTX have almost coplanar structure (torsional angle 6°).

The van der Waals energy between the PTX and pristine CNT and *f*-CNTs was calculated and shown in Fig. 6a. It can be seen, at the start time of simulation there is little van der Waals attraction between PTX molecules and CNTs, but the van der Waals energy decreased when the PTX molecules approached the CNT surface. This finding confirms that the drug molecules

Fig. 6 a) Van der Waals (Leanard-Jones, LJ) interactions between drug molecules and CNT(red), COOH-CNT(blue), AMINE-CNT(pink), and PEG-CNT(green). b) Representative snapshots of drug adsorbing on PEG-CNT with respect the changes in the van der Waals energy values (In the first 15 ns simulation)

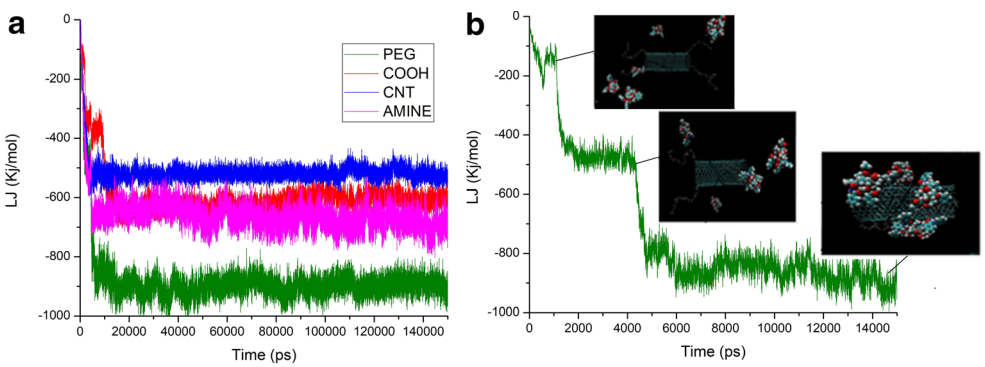

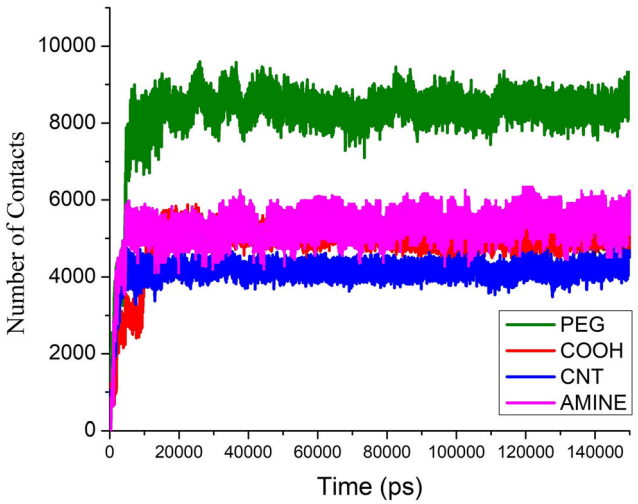

Fig. 7 Number of atomic contacts between PTX and CNT(red), COOH-CNT(blue), AMINE-CNT(pink), and PEG-CNT(green)

can be adsorbed spontaneously on the surface of CNT in aqueous solutions. Figure 6b also shows some representative conformations in the first 15 ns simulation trajectories. These conformations clearly indicate that the absorption of the drug leads to a decrease in van der Waals energy.

Mousavi et al. mentioned that the van der Waals interaction is one of the main interactions in the delivery of PTX molecules [11]. As a result, we conclude that systems with the lower LJ value have higher efficiency in drug delivery cellular uptake. Figure 6 illustrates that the van der Waals interactions in the PEG-CNT system are stronger than the other systems. It indicates that in this system, the PTX molecules interact more favorably with stronger affinity.

The number of atomic contacts between the PTX molecules and the pristine CNT and *f*-CNTs was calculated, by using:

$$N_c(t) = \sum_{i=1}^{N_{CNT}} \sum_{j=1}^{N_{PTX}} \int_{r_i}^{r_i+0.6\ nm} \delta\big(r(t) - r_j(t)\big) dr \qquad (6)$$

Here, N_{CNT} and N_{PTX} are the total number of CNT and PTX atoms respectively, and r_j is the distance of j^{th} atom of PTX from i^{th} atom of the CNT. The δ function ensures counting of all drug atoms within 0.6 *nm* from CNT atoms. Figure 7 shows the number of atomic contacts between the PTX molecules and the pristine CNT and *f*-CNTs. This figure shows that by adsorption of drug, the number of contacts in all systems significantly increased, and at the end of simulation, the number of these contacts for PEG-CNT, AMINE-CNT, COOH-CNT, and pristine CNT are 7900, 5000, 4900, and 4300, respectively. These values show that the number of contacts with drug molecules in *f*-CNT systems are more than pristine CNT, which suggest that the functional groups play an important role in the drug adsorption.

There is a significant correlation between the number of contact values and other obtained results that have a good agreement with the results of Lay et al. [8] and vividly show that the PEG group can greatly enhance the efficiency of CNT in PTX delivering.

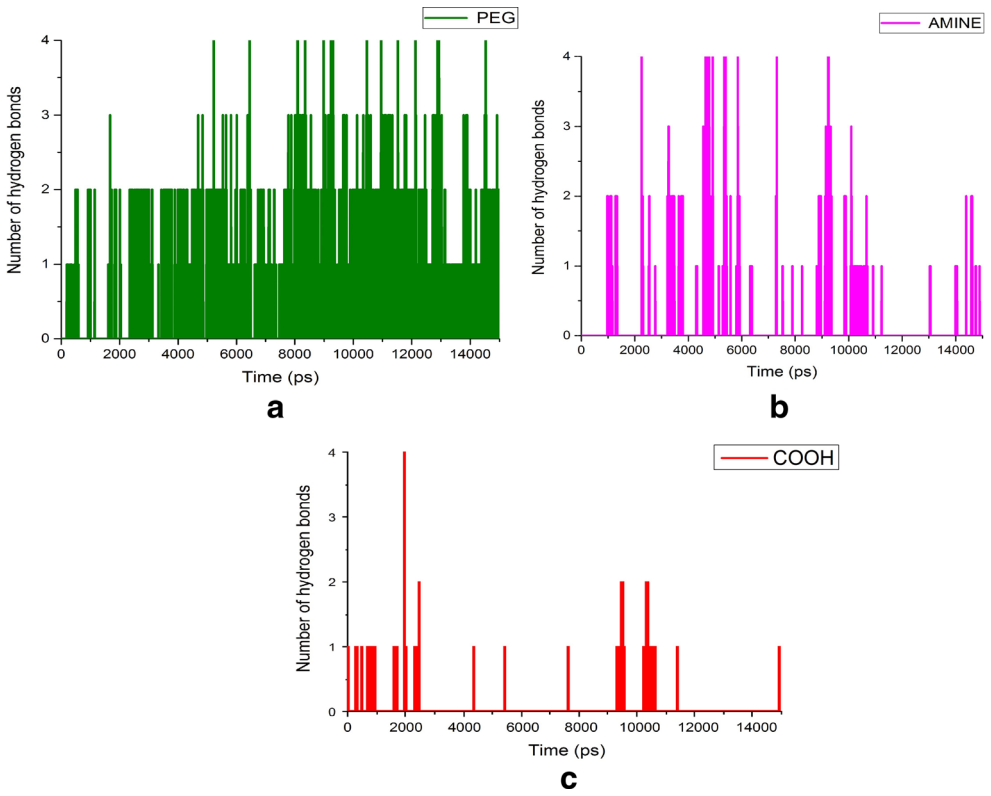

Fig. 8 Number of hydrogen bonds between drug molecules and *f*-CNTs (a: PEG-CNT, b: AMINE-CNT, and c: COOH-CNT)

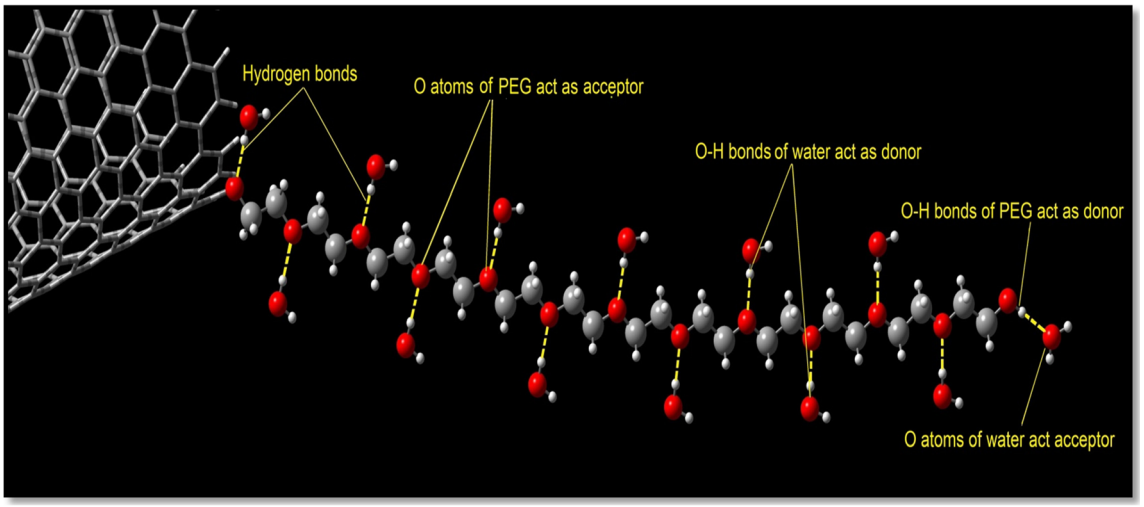

Fig. 9 Schematic of intermolecular hydrogen bonding that occurs between PEG functional group with water molecules

Furthermore, it should be mentioned that some adsorbed drug molecules can be desorbed from the CNT surface and then re-adsorbed to CNT later to take proper orientation. For this reason, the number of contact curves fluctuates in the first 5 ns of simulation and then stabilizes (see Fig. 7) [18].

To further clarify the effect of functional groups on drug adsorption, we calculate the RDF and the number of HBs between functional groups and PTX. The RDF of PTX around the functional groups shows that the intensity of the interactions between this group and drug molecules are markedly raised for the PEG group (Fig. S4).

The number of HBs between PTX molecules and functional groups are shown in Fig. 8. As expected, the HBs between PEG group and PTX molecules are more than COOH and AMINE groups. According to the theoretical and experimental evidence, these HBs can enhance the capacity of adsorbance and increase the stability of drug [26].

Solubility

The main purpose of functionalization of CNTs is to improve the dispersion of CNTs in aqueous solutions [2]. In the present work, CNT was functionalized by using three functional groups in four centers in the same sites at the end of the CNT (all *f*-CNT shown in Fig. 1). These groups were selected because they represent a high water-solubility and good biocompatibility. Different parameters including the number of HBs between *f*-CNT and water molecules, solvation free energy, solvent accessible surface area (SASA), and number of water molecules within 3.5 *Å* region from surface of CNT have been calculated in order to evaluate the effect of functional groups on the solubility of CNTs.

HB undoubtedly is one of the most vital and interesting interactions that frequently occurs in nature which can affect many biochemical processes. Hydrogen bonding leads to considerable change in the properties of liquids, solids or large clusters. Since HB is a very important phenomenon in nature, there are many studies for understanding the nature of HBs [27, 28]. The solubility of organic structures can usually be controlled by forming intermolecular hydrogen bonds between water molecules and their functional groups [29]. In our investigated systems, intermolecular HBs can be formed between heteroatoms of *f*-CNTs and water molecules. Figure 9 shows an overview of the intermolecular hydrogen bonding that occurs between PEG functional groups and solvent molecules. As can be seen, the PEG group in HB can act as both an acceptor and a donor, so that its oxygen atoms act as acceptor and the terminal hydroxyl groups act as donor (see Fig. 9).

The number of HBs between the water molecules and the *f*-CNT were calculated and presented in Fig. S5. Comparison with fCNTs indicates that the number of HBs in the PEG-CNT system (Fig. S5a) is greater than the COOH-CNT and AMINE-CNT. This result show that the PEG groups not only increase the adsorption capacity, but also enhance drug solubility in aqueous solution.

One of the most important developments in computational chemistry is solvation free energy calculations of molecules accurately using thermodynamic perturbation. Solvation free energy, ΔG_{sol}, for CNT and *f*-CNT was calculated and represented in Table 1. Among the four systems, the highest solvation free energy was found in the PEG-CNT system due to greater HBs formation between PEG and water molecules.

Table 1 Computed solvation free energies

Name	Free energy (kJ mol^{-1})
CNT	−1829.63
PEG-CNT	−2159.35
COOH-CNT	−1907.84
AMINE-CNT	−1911.06

The SASA is the surface area of compounds which is accessible to contact with solvent molecules [30]. According to the first algorithm proposed by Lee and Richards [31], SASA of an atom is the area on the surface of a sphere of radius R, on each point of which the center of a solvent molecule can be placed in contact with this atom without penetrating any other atoms of the molecule. The radius R is given by the sum of the van der Waal's radius of the atom and the chosen radius of the solvent molecule. An approximation of this area is computed by this program using the formula:

$$SASA = \sum \left[\frac{R}{\sqrt{R^2 - Z_i^2}} \right] L_i.D \quad (7)$$

$$D = \Delta Z/2 + \Delta' Z \quad (8)$$

Where L_i is the length of the arc drawn on a given section i, Z_i is the perpendicular distance from the center of the sphere to the section i, ΔZ is the spacing between the sections, and $\Delta' Z$ is $\Delta Z/2$ or R - Z_i, whichever is smaller. Summation is over all the arcs drawn for the given atom [32].

Figure S6 shows the hydrophobic SASA for all of the investigated systems. Average values of the hydrophobic SASA for CNT, COOH-CNT, AMINE-CNT, and PEG-CNT are 59.45, 53.32, 51.99, and 62.92 nm^2, respectively. The higher values for the PEG-CNT in comparison to the other CNTs confirm that PEG-CNT system has more surface area, which is available to interact with water molecules.

Furthermore, Fig. S6 indicates that the hydrophobic SASA for all systems are decreased by increasing the time. The reason for this decline can be related to formation of the π-π interactions between the hydrophobic surface of CNT and aromatic rings of the drug molecules.

Finally, the number of water molecules within 3.5 Å of CNTs for all systems as a function of time are depicted in Fig. S7. Water molecules form a hydration shell around CNT surfaces, which can be affected by the adsorption of drug on the sidewalls of CNTs. This means that the drug drives away the water molecules from CNT surface leading to the formation of strong π-π interactions. For this reason, the number of water molecules were decreased in all of the investigated systems. Also, this figure shows that the number of water molecules in the PEG-CNT system are almost more than the other systems. This results indicates that this system was more soluble in water solution.

The obtained results from the number of HBs, free energy, SASA, and the number of water molecules are in agreement and show that functionalization of CNT increases its solubility. Also, these parameters confirm that the PEG-CNT system has the highest solubility.

Conclusions

MD simulations were performed to investigate the adsorption mechanism of the PTX drug on a pristine CNT and *f*-CNTs in aqueous solution. In this work, CNT has been functionalized with COOH, PEG (with 12 monomers), and CH2NH2 in four centers in the same sites at the edges of the CNT. Radial distribution functions, van der Waals energy, the number of contacts and the number of hydrogen bonds are analyzed to understand the nature of the main interactions between PTX molecules and CNTs. The obtained results show that the PTX drug can be adsorbed on CNTs by π-π stacking, which was formed between the PTX and surfaces of CNTs, and also by formation of polar interactions between drug and functional groups of *f*-CNTs. Results of van der Waals energy and the number of contacts indicate that the PEG-CNT system has the best performance in drug adsorption.

The number of hydrogen bonds, solvent accessible surface area, and the number of water molecules around the CNT show that functionalization strongly increases the solubility of CNT. This fact can be attributed to the formation of hydrogen bonds between functional groups of CNTs and water molecules. Furthermore, the PEG-CNT system has the highest solubility in water solution.

References

1. Cragg GM, Grothaus PG, Newman DJ (2009) Impact of natural products on developing new anti-cancer agents. Chem Rev 109: 3012–3043
2. Kushwaha S, Rastogi A, Rai A, Singh S (2012) Novel drug delivery system for anticancer drug: a review. SphinxsaiCom 4:542–553
3. Vashist SK, Zheng D, Pastorin G, et al. (2011) Delivery of drugs and biomolecules using carbon nanotubes. Carbon 49:4077–4097
4. Rowinsky EK, Donehower RC (1995) Paclitaxel (taxol). N Engl J Med 332:1004–1014
5. Ma P, Mumper RJ (2013) Paclitaxel nano-delivery systems: a comprehensive review. J Nanomed Nanotechnol 4:1000164
6. Sun H, She P, Lu G, et al. (2014) Recent advances in the development of functionalized carbon nanotubes: a versatile vector for drug delivery. J Mater Sci 49:6845–6854. doi:10.1007/s10853-014-8436-4
7. Jain KK (2012) Advances in use of functionalized carbon nanotubes for drug design and discovery. Expert Opin Drug Discov:1–9. doi:10.1517/17460441.2012.722078
8. Lay CL, Liu HQ, Tan HR, Liu Y (2010) Delivery of paclitaxel by physically loading onto poly (ethylene glycol)(PEG)-graftcarbon nanotubes for potent cancer therapeutics. Nanotechnology 21: 65101
9. Arsawang U, Saengsawang O, Rungrotmongkol T, et al. (2011) How do carbon nanotubes serve as carriers for gemcitabine transport in a drug delivery system? J Mol Graph Model 29:591–596
10. Li Z, Tozer T, Alisaraie L (2016) Molecular dynamics studies for optimization of noncovalent loading of vinblastine on single-walled carbon nanotube. J Phys Chem C 120:4061–4070

11. Mousavi SZ, Amjad-Iranagh S, Nademi Y, Modarress H (2013) Carbon nanotube-encapsulated drug penetration through the cell membrane: an investigation based on steered molecular dynamics simulation. J Membr Biol 246:697–704
12. Liu Z, Chen K, Davis C, et al. (2008) Drug delivery with carbon nanotubes for in vivo cancer treatment. Cancer Res 68:6652–6660
13. http://www.jcrystal.com/products/wincnt/, Nanotube Modeler, JCrystalSoft Ed., 2004–2005
14. Maata J, Vierros S, Van Tassel PR, Sammalkorpi M (2014) Size-selective, noncovalent dispersion of carbon nanotubes by PEGylated lipids: a coarse-grained molecular dynamics study. J Chem Eng Data 59:3080–3089
15. Schmidt MW, Baldridge KK, Boatz JA, et al. (1993) General atomic and molecular electronic structure system. J Comput Chem 14: 1347–1363
16. Ghadamgahi M, Ajloo D (2015) Molecular dynamics insight into the urea effect on Tretinoin encapsulation into carbon nanotube. J Braz Chem Soc 26:185–195
17. Brooks BR, Brooks CL, MacKerell AD, et al. (2009) CHARMM: the biomolecular simulation program. J Comput Chem 30:1545–1614
18. He Z, Zhou J (2014) Probing carbon nanotube–amino acid interactions in aqueous solution with molecular dynamics simulations. Carbon 78:500–509
19. Zaboli M, Raissi H (2016) The influence of nicotine on pioglitazone encapsulation into carbon nanotube: the investigation of molecular dynamic and density functional theory. J Biomol Struct Dyn 1102: 1–15. doi:10.1080/07391102.2016.1152565
20. Zoete V, Cuendet MA, Grosdidier A, Michielin O (2011) SwissParam: a fast force field generation tool for small organic molecules. J Comput Chem 32:2359–2368
21. Jorgensen WL, Chandrasekhar J, Madura JD, et al. (1983) Comparison of simple potential functions for simulating liquid water. J Chem Phys 79:926–935
22. Kirkwood JG (1935) Statistical mechanics of fluid mixtures. J Chem Phys 3:300–313
23. Hess B, Kutzner C, Van Der Spoel D, Lindahl E (2008) GROMACS 4: algorithms for highly efficient, load-balanced, and scalable molecular simulation. J Chem Theory Comput 4:435–447
24. Berendsen HJC, JPM P, van Gunsteren WF, et al. (1984) Molecular dynamics with coupling to an external bath. J Chem Phys 81:3684–3690
25. Humphrey W, Dalke A, Schulten K (1996) VMD: visual molecular dynamics. J Mol Graph 14:33–38
26. Izadyar A, Farhadian N, Chenarani N (2016) Molecular dynamics simulation of doxorubicin adsorption on a bundle of functionalized CNT. J Biomol Struct Dyn 34:1797–1805
27. Toosy NKA, Raissi H, Zaboli M (2016) Theoretical calculations of intramolecular hydrogen bond of the 2-amino-2, 4, 6-cycloheptatrien-1-one in the gas phase and solution: substituent effects and their positions. J Theor Comput Chem 15:1650063
28. Khoshbin Z, Raissi H, Zaboli M (2015) The DFT and MP2 based computational scrutiny on blue-shifted H–F stretching vibrational frequencies in hydrogen-fluoride complexes with nitriles: Insights into the decisive role of intermolecular hydrogen bonding (IMHB) in ground and electronic excited states. Arab J Chem doi:10.1016/j.arabjc.2015.06.003
29. Small PA (1953) Some factors affecting the solubility of polymers. J Appl Chem 3:71–80
30. Faujan NH, Karjiban RA, Kashaban I, et al. (2015) Computational simulation of palm kernel oil-based esters nano-emulsions aggregation as a potential parenteral drug delivery system. Arab J Chem doi:10.1016/j.arabjc.2015.03.003
31. Lee B, Richards FM (1971) The interpretation of protein structures: estimation of static accessibility. J Mol Biol 55:379–400
32. Ausaf Ali S, Hassan I, Islam A, Ahmad FA (2014) Review of methods available to estimate solvent-accessible surface areas of soluble proteins in the folded and unfolded states. Curr Protein Pept Sci 15:456–476